

See discussions, stats, and author profiles for this publication at: <https://www.researchgate.net/publication/346547644>

# Morphological evolution of silica scales in the freshwater genus *Synura* (Stramenopiles)

Article in *Journal of Phycology* · November 2020

DOI: 10.1111/jpy.13093

---

CITATIONS

0

---

READS

61

3 authors, including:



[Peter A. Siver](#)

Connecticut College

168 PUBLICATIONS 2,845 CITATIONS

[SEE PROFILE](#)



[Pavel Skaloud](#)

Charles University in Prague

149 PUBLICATIONS 2,345 CITATIONS

[SEE PROFILE](#)

Some of the authors of this publication are also working on these related projects:




Hi Magdalena, [View project](#)




Terricolous Lichens In India (Books) [View project](#)



## MORPHOLOGICAL EVOLUTION OF SILICA SCALES IN THE FRESHWATER GENUS *SYNURA* (STRAMENOPILES)<sup>1</sup>

Iva Jadrná <sup>2</sup>

Department of Botany, Faculty of Science, Charles University, Benátská 2, 128 00 Praha 2, Czech Republic

Peter A. Siver 

Department of Botany, Connecticut College, New Londo 06320-4196, Connecticut, USA

and Pavel Škaloud 

Department of Botany, Faculty of Science, Charles University, Benátská 2, 128 00 Praha 2, Czech Republic

A high degree of morphological variability is expressed between the ornately sculptured siliceous scales formed by species in the chrysophycean genus, *Synura*. In this study, we aimed to uncover the general principles and trends underlying the evolution of scale morphology in this genus. We assessed the relationships among thirty extant *Synura* species using a robust molecular analysis that included six genes, coupled with morphological characterization of the species-specific scales. The analysis was further enriched with addition of morphological information from fossil specimens and by including the unique modern species, *Synura punctulosa*. We inferred the phylogenetic position of the morphologically unique *S. punctulosa*, to be an ancient *Synura* lineage related to *S. splendida* in the section *Curtispinae*. Some morphological traits, including development of a keel or a labyrinth ribbing pattern on the scale, appeared once in evolution, whereas other structures, such as a hexagonal meshwork pattern, originated independently several times over geologic time. We further uncovered numerous construction principles governing scale morphology and evolution, as follows: (i) scale roundness and pore diameter decreased during evolution; (ii) elongated scales became strengthened by a higher number of struts or ribs; (iii) as a consequence of scale biogenesis, scales with spines possessed smaller basal holes than scales with a keel and; and (iv) the keel area was proportional to scale area, indicating its potential value in strengthening the scale against breakage.

**Key index words:** chrysophytes; construction principles; microalgae; molecular; morphology; phylogeny; silica scales; *Synura punctulosa*; synurophytes; ultra-structure

**Abbreviations:** BIC, Bayesian information criterion; MCMC, Markov Chain Monte Carlo; mt, mitochondrial; NMDS, non-metric multidimensional scaling; nu, nuclear; psaA, photosystem I P700 chlorophyll a apoprotein A1; pt, plastid; SDV, silica deposition vesicle

---

Every day, we observe inorganic and living objects with a vast array of shapes, patterns, structures, and colors. Morphological variability expressed in living organisms is often explained by a random and passive tendency to increase complexity, constrained by physical and mechanical laws, and ultimately shaped by natural selection. Examples of such morphological diversification are those driven by sexual selection or social competition in plants and their pollinating insects (Castellanos et al. 2006, Whittall and Hodges 2007, Quesada-Aguilar et al. 2008), eccentrically colored birds (Endler and Day 2006, Rubenstein and Lovette 2009, Maia et al. 2013), and fishes such as cichlids (Elmer et al. 2010, Arbour and López-Fernández 2013, Feilich 2016).

Compared to the macroscopic world, studies explaining morphological diversity among small, largely microscopic, eukaryotic organisms are few. Despite their small size, protists are extremely disparate with respect to their physiology and genetic makeup, and some groups display incredible morphological diversity. Among the most morphologically diversified protists are those organisms that construct structures using organic (e.g., glycoproteins and cellulose) or inorganic (e.g., silica, calcium, and strontium) materials.

*Synura* (Synurales, Chrysophyceae, and Stramenopiles) is a genus of freshwater algae consisting of species that form motile colonies, where each cell is covered with a highly organized series of overlapping siliceous scales (Starmach 1985, Leadbeater 1990, Siver 2015). The highly sculptured scales are positioned in spiral rows that can be traced from the flagellar end of the cell, around the body of the organism, to the posterior end. The great diversity

---

<sup>1</sup>Received 18 June 2020. Revised 13 October 2020. Accepted 17 October 2020.

<sup>2</sup>Author for correspondence: e-mail jadrnai@natur.cuni.cz.  
Editorial Responsibility: R. Wetherbee (Associate Editor)

of scale ornamentation was initially revealed with transmission electron microscopy in the 1950s (Manton 1955, Petersen and Hansen 1956, Fott and Ludvík 1957) and later with scanning electron microscopy (Hartmann and Steinberg 1986, Siver 1987). Scales have a bilateral symmetry, range in length up to approximately 10  $\mu\text{m}$ , and their designs are species-specific. All scales possess a basal plate perforated with pores, an upturned rim usually encircling half to two-thirds of the scale, and either a forward projecting spine or a raised elongated ridge positioned on the middle of the scale referred to as the median keel (Fig. 1). In addition to variability between species, environmental conditions and position on the cell body influence the morphology of *Synura* scales. *Synura* species are found under a wide range of ecological conditions (Kristiansen 1979, 2008), which, in turn, can result in subtle differences in scale morphology. Phenotypic plasticity of scale shape is also impacted by environmental stress (Sandgren et al. 1996, Saxby-Rouen et al. 1997). A number of studies have documented a decline in scale and spine length with increasing temperature (Martin-Wagenmann and Gutowski 1995, Gutowski 1996, Řezáčová-Škaloudová et al. 2010), noting a shift toward more oval to elongate shapes (Pichrtová and Němcová 2011). Long-term cultivation under both lower temperature and light conditions can also result in a decrease in scale size (Němcová et al. 2010), and cells growing for extended periods in culture often begin to produce less silicified scales (Leadbeater 1986, Martin-Wagenmann and Gutowski 1995). Suboptimal pH conditions have also been shown to impact scale morphology (Gavrilova et al. 2005), including the degree of secondary ornamentation and width of the upturned rim (Němcová and Pichrtová 2012).

Another factor influencing scale shape and design is the position of the scale on the cell surface (Asmund 1968, Siver 1987). Scales can be divided into apical, body, and caudal scales depending on where they are found along the longitudinal axis of the cell (Kristiansen 1979). The majority of scales

forming the scale coat are body scales, found over most of the length of the cell and consisting of similar features. Apical and caudal scales, found on the flagellar and posterior ends of the cell, respectively, are shaped differently from body scales in order to more effectively cover the changing shape of the cell. Often, apical scales are smaller, more rounded, and with longer spines, whereas caudal scales become more elongated with shorter spines (Kristiansen 1979, Siver 1987).

Despite small degrees of scale variability, the overall morphological structure of scales is a conservative, species-specific, and taxonomically relevant trait that has been successfully used to delineate between *Synura* taxa (Jo et al. 2016). Petersen and Hansen (1956) originally proposed to divide the genus into two sections, *Petersenianae* and *Spinosaes*, according to the presence or absence of the median keel. Despite later taxonomic rearrangements within the genus, the presence of a keel versus a projecting spine has proven a most valuable character in understanding the phylogenetic arrangement of species (Škaloud et al. 2014, 2020, Siver et al. 2015, Jo et al. 2016). Péterfi and Momeu (1977) proposed a third section, *Lapponica*, to accommodate one species with very different scales that lacked both a keel and a spine. These authors also proposed the section *Synura* to replace section *Spinosaes* (= *Uvellae*) and further divided section *Synura* into two series, *Synura* and *Splendidae* (Péterfi and Momeu 1977). Additional phylogenetic relationships were suggested by Wee (1997), and Kristiansen and Preisig (2007) noted three sections within the genus, *Lapponica*, *Petersenianae*, and *Synura*. More recently, section *Lapponica* consisting solely of *Synura lapponica* was revealed to belong in the genus *Tessellaria* (Škaloud et al. 2013), which was later renamed as *Neotessella* (Jo et al. 2016). Multiple studies using a combination of ecological, physiological, morphological, and molecular approaches have further improved our understanding of relationships between species in *Synura* (Boo et al. 2010, Škaloud et al. 2012). Škaloud et al. (2013) confirmed section *Petersenianae* (= *Peterseniae*)

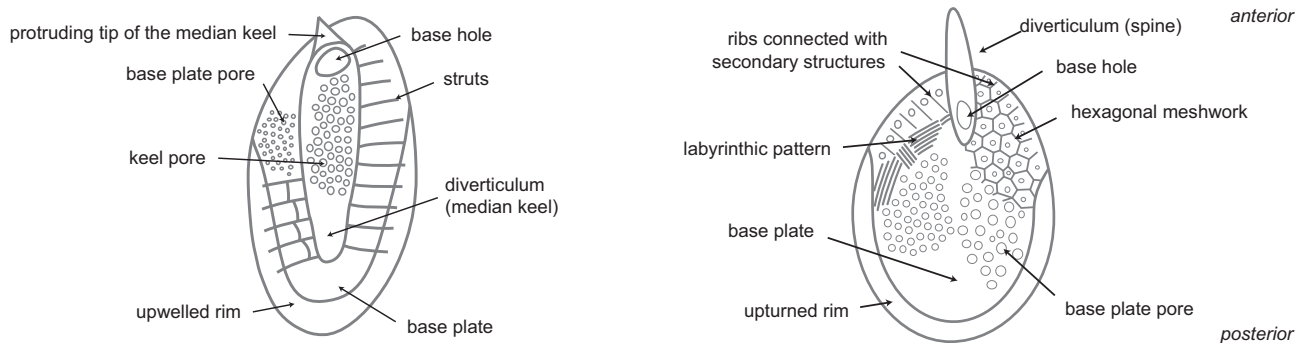


FIG. 1. The outline of siliceous *Synura* scales showing its major morphological features. Typical body scales with the spine (left) and with the median keel (right) are presented.

as clearly being monophyletic, but pointed out that the section containing species with projecting spines, namely *Uvellae* or *Synura*, was phylogenetically and morphologically diverse. As a result, Škaloud et al. (2013) proposed further classification of taxa with spines into the four sections, *Spinosaes*, *Echinulatae*, *Splendidae*, and *Uvellae*. In other recent phylogenetic works, *Synura* was divided into either two sections *Synura* and *Petersenianaes* (Siver et al. 2015), or into three sections *Synura*, *Curtispinaes*, and *Petersenianaes* (Jo et al. 2016). In summary, formation of a scale bearing a spine versus a keel, as originally proposed by Petersen and Hansen (1956), was an important event in the evolution of *Synura* that is a primary character used to distinguish between the currently 55 recognized taxa (Němcová et al. 2008, Jo et al. 2016, Pusztai et al. 2016, Siver and Lott 2016, Siver et al. 2018).

The goal of the current study was to uncover evolutionary patterns in scale design within *Synura* using a suite of morphological characters and fossil evidence in relation to a molecular-based phylogenetic framework. Specifically, our goal was to uncover overarching principles and trends shaping the evolution of scale morphology over geologic time. As part of our study, we have included new information on a key species, *Synura punctulosa*, a potential missing link in the evolution of the genus, and all known fossil species.

#### MATERIAL AND METHODS

*Collection, isolation, and cultivation.* *Synura punctulosa* was sampled in Chanty-Mansijsk (Ханты-Мансийск) region in south-western Siberia, Russia, during the beginning of June 2018. Specifically, the strains were collected in a flooded valley of the River Matkinskaya (Маткинская, 61°01'10.1" N 68°05'02.4" E). Standard measurements of abiotic factors of the sampling site were performed using a combined pH/conductivity meter (WTW 340i; WTW GmbH, Weilheim, Germany). At the time of collection, the temperature was 11.9°C, pH was 7.1 and the specific conductivity measured 65  $\mu\text{S} \cdot \text{cm}^{-1}$ . In the effort to establish monoclonal algal cultures, individual colonies were isolated by micropipetting and transferred into a 96-well plate filled with WC liquid medium (Boenigk et al. 2006). The algae were cultivated at approximately 15°C under a constant illumination of 40  $\mu\text{mol} \cdot \text{m}^{-2} \cdot \text{s}^{-1}$  (TLD 18W/33 fluorescent lamps, Philips, Amsterdam, the Netherlands). After 14 d, the cultures were inoculated into 50 mL Erlenmeyer flasks filled with the same medium (Pusztai et al. 2016).

*Sequencing and phylogenetic analyses.* For DNA isolation, 200  $\mu\text{L}$  of cultured algae was harvested using centrifugation and frozen in PCR strips at  $-80^\circ\text{C}$ . Then, 30  $\mu\text{L}$  of InstaGene matrix (Bio-Rad Laboratories, Hercules, CA, USA) was added to the pellet. The samples were vortexed, incubated at 56°C for 30 min, and heated at 99°C for 8 min. Afterward, the supernatant was directly used as a PCR template.

We amplified six molecular markers (nu SSU rDNA, nu LSU rDNA, nu ITS rDNA, pt LSU rDNA, pt *rbL*, and pt *psaA*) to infer a robust phylogenetic analysis, using the following primers. The nu SSU rDNA gene was amplified with the primers 18S\_F and 18S\_R (Katana et al. 2001), and the nu

LSU rDNA using the combination of primers 28S\_25F, 28S\_2812R (Jo et al. 2011), and 28S\_1435R (Pusztai et al. 2016). The pt LSU rDNA was amplified with primers 23S\_Syn\_AF and 23S\_Syn\_928R (Škaloud et al. 2020). The amplification of nu ITS rDNA was performed using newly designed primers Chryso\_ITS\_F (5'-ATC ATT TAG AGG AAG GTG A-3') and Chryso\_ITS\_R (5'-GCT TCA CTC GCC GTT ACT-3'). The pt *rbL* gene was amplified using primers *rbL\_R3* (Jo et al. 2011) and *rbL\_chrys\_F2* (Škaloudová and Škaloud 2013). Finally, the pt *psaA* gene was amplified using the primers *psaA130F* and *psaA1760R* (Yoon et al. 2002).

All PCRs were prepared in a 10  $\mu\text{L}$  volume consisting of 6.5  $\mu\text{L}$  H<sub>2</sub>O, 2  $\mu\text{L}$  buffer, 0.2  $\mu\text{L}$  of each forward and reverse primers, 0.1  $\mu\text{L}$  MyTaq polymerase, and 1  $\mu\text{L}$  DNA template. The PCR products were quantified on 0.8% agarose gel stained with ethidium bromide and purified using MagJET Magnetic Bead-based Nucleic Acid Purification (ThermoFisher Scientific, Waltham, MA, USA). The purified amplification products were sequenced in Macrogen Europe (Amsterdam, Netherlands).

New sequences were manually checked using SeqAssem v. 9 (Hepperle 2004), added to the alignment published by Jo et al. (2016), and supplemented by several sequences deposited in GenBank database. Accession numbers of all analyzed sequences are listed in Supplementary information (Table S1 in the Supporting Information). Multiple alignment was built for the following analyses using MEGA5 (Tamura et al. 2011), including 64 strains of *Synurales* and two strains of *Neotessella* that were used as the outgroup. The sequences were aligned using MAFFT version 7 under the Q-INS-I strategy (Katoh et al. 2019) with the only exception of nu ITS2 rDNA, which was aligned and built according to its secondary structure. The sequences of nu ITS2 rDNA were modeled with The ITS2 Database V (Ankenbrand et al. 2015) to assure its homology and again manually checked for obvious aligning errors. DNA alignments are freely available on Mendeley Data: <http://dx.doi.org/10.17632/rh2t2zgf7pz.1>.

Suitable partition-specific substitution models were selected using the Bayesian information criterion (BIC) implemented in jModelTest 2.1.10 (Darriba et al. 2012). The following models with the lowest BIC scores were selected: (1) HKY + I+G for nu SSU rDNA and nu ITS1 rDNA, (2) GTR + I+G for nu LSU rDNA, pt LSU rDNA, and nu ITS2 rDNA, the first and third codon position of the pt *rbL* and pt *psaA* genes, respectively, (3) JC + I for the second and (4) GTR + G for third codon position of the pt *rbL* gene, (5) GTR + I for the first and (6) HKY + I for the second codon position of the pt *psaA* gene, and (7) SYM + G for nu 5.8S rDNA. Each part of the alignment was checked and trimmed with Gblocks software (Castresana 2000). The loci of nu SSU rDNA, nu LSU rDNA, pt LSU rDNA, nu ITS1 rDNA, nu 5.8S rDNA, nu ITS2 rDNA, pt *rbL*, and pt *psaA* were concatenated, yielding a robust alignment of 9,680 bases.

The phylogenetic tree was first inferred using RaxML BlackBox with 250 replicates under the GTR Gamma + model with partitions (Stamatakis 2014) and rapid bootstrapping as implemented in the CIPRES Science Gateway (Miller et al. 2010). Second, we repeated the phylogenetic analysis with Bayesian inference (BI) using MrBayes version 3.2.1 (Ronquist et al. 2012). Three independent Markov Chain Monte Carlo (MCMC) chains were run for 3  $\times$  100 million generations, sampling every 1,000 generation after 25% burn-in and checked for stationarity and convergence of independent chains. The resulting tree was then compared with the tree based on Bayesian framework in BEAST v1.10.4 (Suchard et al. 2018) used for final phylogenetic analyses. Lognormal relaxed clock models were applied for the partitions and a birth-death diversification process

was selected as a prior on the distribution of node heights. For temporal calibration of the phylogeny, we used time constraints based on well-preserved fossil scales found in geological deposits in Northern Canada, the Giraffe (Siver et al. 2015) and Wombat (Siver et al. 2013a) cores, as follows: (i) the lineage consisting of *Synura uwella* and *S. splendida* (Giraffe core), (ii) the lineage of *S. curtispina* and *S. longitubularis* (Giraffe core), and (iii) the stem of all *Petersenianae* taxa including *S. macracantha* (Wombat core). The splits were adjusted on an offset of either 48 (Giraffe core) or 83 Ma (Wombat core) with the mean of 8.0 and a standard deviation of 6.0, which represent the minimal estimated age of fossils. The MCMC analyses were run for  $5 \times 100$  million generations, sampling every 500,000 generation after 1.5 million generations removed as a burn-in. We checked the parameter-estimated convergence with Tracer v1.7.1. (Rambaut et al. 2018) and then constructed the final chronogram with age estimation for all nodes. Trees were visualized using FigTree ver.1.4.2. (Rambaut 2016).

**Morphological investigation of silica scales.** A total of 30 *Synura* species that are well defined using both molecular and morphological characters were used for the morphological study, including *Synura americana*, *S. asmundiae*, *S. bjoerkii*, *S. borealis*, *S. conopea*, *S. curtispina*, *S. echinulata*, *S. glabra*, *S. heteropora*, *S. hibernica*, *S. kristiansenii*, *S. lanceolata*, *S. laticarina*, *S. leptorhabda*, *S. longitubularis*, *S. macracantha*, *S. macropora*, *S. mammillosa*, *S. mollispina*, *S. multidentata*, *S. petersenii*, *S. punctulosa*, *S. soroconopea*, *S. sphagnicola*, *S. spinosa*, *S. splendida*, *S. sungminbooi*, *S. synuroidea*, *S. truttae*, and *S. uwella* (Fig. 2). Images of scales from 29 of the *Synura* species (all except *S. punctulosa*) were taken largely from our personal database or from records contained in the chrysophytes.eu database (Škaloud et al. 2013) that included verified species identifications. For most species, we used images of actively growing specimens from the same cultures used for molecular analyses. Cultures and field collections of *Synura punctulosa* were initially examined with an Olympus BX 51 light microscope equipped with Nomarski interference contrast, and then, the scales were characterized using images taken with a JEOL 1011 transmission electron microscope (TEM) equipped with a Veleta CCD camera and operated with Olympus Soft Imaging Solution Software GmbH (Münster, Germany). Samples of *S. punctulosa* were prepared for observation with TEM by adding several drops from actively growing cultures onto Formvar-coated copper grids, allowed to dry, gently washed with distilled water, and finally redried.

We analyzed 44 morphological traits for all 30 species as defined in Škaloud et al. (2014), forty of which are quantitative (Table S2 in the Supporting Information). In an effort to more fully cover all major morphotypes, we also included scales from fossil specimens of *Synura macracantha*, *S. nygaardii*, *S. recurvata*, and *S. cronbergiae* uncovered from the Giraffe Pipe and Wombat fossil sites in Northern Canada (Siver and Wolfe 2005, Siver et al. 2013a,b). For consistency across species, we selected only body scales for all morphometric analyses. All measurements were obtained using ImageJ version 1.46r (Rasband 1997) on a minimum of ten scales per species, and all traits were analyzed only if the homology derived from the similar biogenesis was reliable. We included three measurements of mean pore size depending on their position on the scale: (1) base plate pores excluding those under the keel and the hexagonal meshwork pattern (labeled as base plate pores on Fig. 1); (2) base plate pores within the hexagonal meshwork pattern (Fig. 1); (3) pores on the base of the keel (labeled as keel pores on Fig. 1). In addition to width, the length of the keel was divided into (i) that portion attached to the base plate; (ii) an estimate of the length of the portion of the keel projecting beyond the base hole; and (iii) the total length (Fig. 1). A few morphological characters,

such as the unique anastomosing ribs of *S. punctulosa* or the ribs under the upturned rim on scales of *S. uwella*, were not included in the analyses.

**Tracing the morphotype evolution of silica scales.** Morphological features of *Synura* scales used to investigate ancestral character states were selected using a combination of scale structure (Fig. 1) and the Synuralean phylogeny, similar to the method used by Čertnerová et al. (2019). A Spearman correlation matrix of all morphological characters was utilized to help select a subset of characters to use in the analysis. Highly correlated characters were identified and removed, and we excluded morphological characters that were not evaluated for at least ten species. All analyses were performed using R v.3.6.1 (R Core Team 2019), and the Bayesian tree trimmed to 30 *Synura* taxa with associated morphological data.

The dataset of non-correlated morphological characters was analyzed by NMDS (non-metric multidimensional scaling) indirect analyses, using the Gower dissimilarity matrix. In addition to the 30 extant *Synura* species, measurements of fossil specimens of *S. macracantha*, *S. nygaardii*, *S. cronbergiae*, and *S. recurvata* were added to the dataset. We projected phylogenetic relationships among *Synura* species into the ordination space to construct a phylomorphospace plot, using the Phytools package in R (Revell 2012). Ancestral states of standardized average values of morphological features were reconstructed using the densityMap, make.simmap, and contMap functions in the Phytools package (Revell 2012), and assuming a Brownian motion model.

## RESULTS

**Phylogenetic analyses.** A time-calibrated phylogenetic tree (Fig. 3) dated the origin of the genus *Synura* in the Early Cretaceous, about 145 mya. Later in the Cretaceous, the genus radiated into the three sections recognized today as *Synura*, *Curtispinae*, and *Petersenianae*. The section *Synura*, consisting solely of the spine-bearing species, *S. uwella*, separated from the rest of the *Synura* species about 111 [100–126] mya. The sections *Curtispinae* and *Petersenianae* split slightly later at about 107 [96–120] mya. Species in section *Curtispinae* retained scales bearing spines, while taxa in section *Petersenianae* developed scales with a keel. *Synura punctulosa*, a species originally described by Balonov (1976), is an ancient lineage most closely aligned with *S. splendida* that originated approximately 79 [53–100] mya, prior to the radiation of the most extant *Synura* species.

**The scale architectural principles.** Correlations between all combinations of morphological traits (Table S3 in the Supporting Information) were used to initially examine constraints of scale formation and to reveal principles of scale structure. Scale characters related to area, perimeter, and length were highly correlated, and the length of the upturned rim was also significantly related to scale perimeter and area. Spine length was related to the length, perimeter, and area of the scale and to the length of the upturned rim, while spine width was clearly linked to scale width. The total length of the keel was additionally correlated with scale perimeter, area and length, the length of the upturned rim, and to the length of the portion of the keel

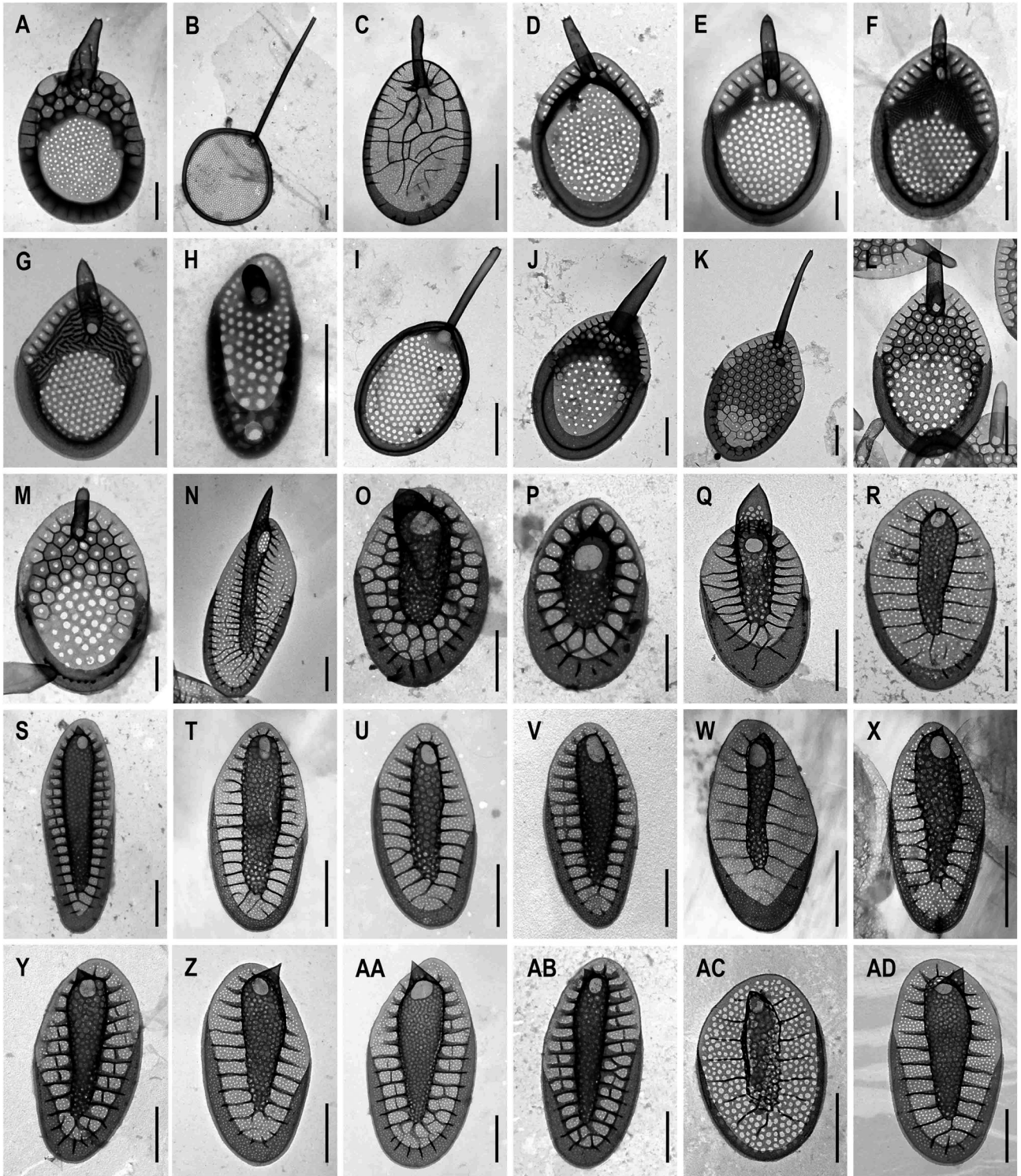


FIG. 2. The scales of *Synura* species evaluated in this study: (A) *S. uvella*, (B) *S. splendida*, (C) *S. punctulosa*, (D) *S. multidentata*, (E) *S. leptorrhabda*, (F) *S. mammosa*, (G) *S. echinulata*, (H) *S. synuroidea*, (I) *S. sphagnicola*, (J) *S. spinosa*, (K) *S. mollispina*, (L) *S. longitubularis*, (M) *S. curtispina*, (N) *S. macracantha*, (O) *S. kristiansenii*, (P) *S. bjoerkii*, (Q) *S. asmundiae*, (R) *S. glabra*, (S) *S. hibernica*, (T) *S. lanceolata*, (U) *S. heteropora*, (V) *S. truttiae*, (W) *S. sungminbooi*, (X) *S. soroconoepa*, (Y) *S. conopea*, (Z) *S. laticarina*, (AA) *S. borealis*, (AB) *S. petersenii*, (AC) *S. macropora*, and (AD) *S. americana*. The scale bars represent 1  $\mu$ m.

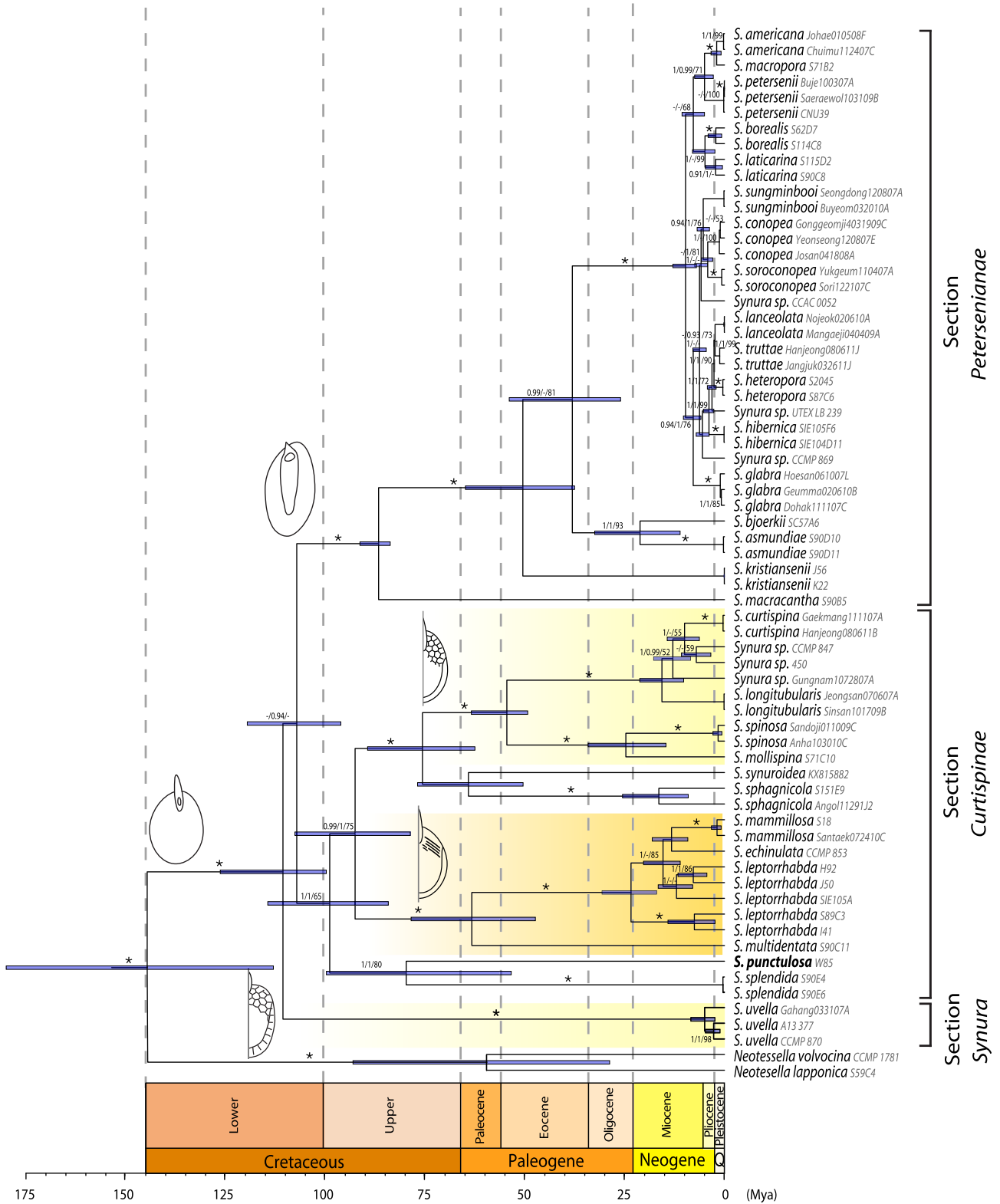


FIG. 3. Multigene time-calibrated phylogenetic tree of the genus *Synura*. Newly molecularly characterized *S. punctulosa* is shown in bold. Values on the tree branches indicate statistical support; posterior node probability inferred with MrBayes (left), BEAST (middle), and maximum likelihood bootstrap (right). Asterisks mark the branches with the highest statistical support (1.00/1.00/100). Geologic time axis is presented in millions of years (Mya). The error bars at the tree nodes represent 95% confidence intervals longer than 2.5 Mya. Landmarks of the *Synura* scale morphology are shown along appropriate branches.

attached to the scale. Although keel width was variable, keel area was related to scale area, and the length of the keel tip was dependent on the scale width. Finally, the number of struts connected to the keel was related to the scale roundness.

**Trends in silica scale evolution.** We combined the NMDS ordination plot of morphological traits with phylogenetic structure to initially investigate trends of scale structure over geologic time within *Synura* (Fig. 4). The genus was clearly divided into two groups, based on the formation of scales with either a projecting spine or a keel, which supports splitting the genus into sections *Petersenianae* and *Synura + Curtispinae*. Fossil specimens of *S. macracantha*, *S. nyaardii*, *S. cronbergiae*, and *S. recurvata* further supported this primary split, but their positions within the ordination plot indicate slight shifts in morphology relative to their closest related modern counterparts, most notably traits

related to scale, spine, and keel size (Fig. 4, A and C). In addition, scale morphologies in the sections *Synura* and *Curtispinae* were more variable than those in the section *Petersenianae* along the first two NMDS axes.

To analyze morphological variation in more detail, the NMDS ordination plots were constructed separately for section *Petersenianae* and for sections *Synura + Curtispinae* using all species included in the study (Fig. 5, A and B). In general, closely related species based on molecular data also had similar morphology. For example, scale morphology for closely related species *S. mammillosa*, *S. echinulata*, and *S. leptorrhabda*, and for *S. spinosa* and *S. mollispina*, overlap in the plot. It is important to remember that the projected morphospaces show scale variability for a limited number of strains and that scale morphospaces are likely larger than indicated by the analyses.

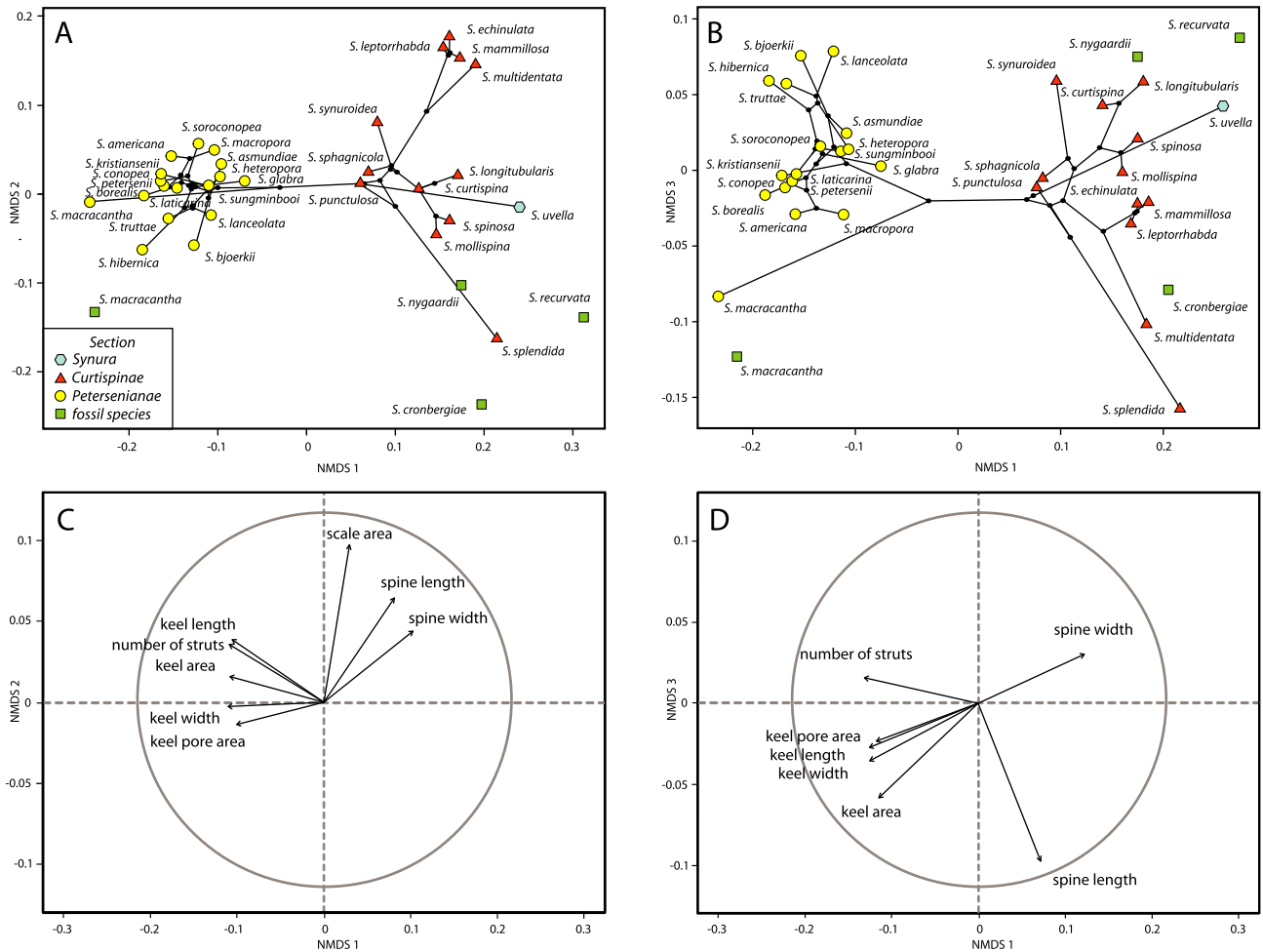


FIG. 4. Phylomorphospace plots representing the projection of phylogenetic relationships among selected *Synura* species onto the ordination diagram (NMDS) based on 32 morphological characters of siliceous body scales. The plots are displayed for NMDS 1 on NMDS 2 (A) and NMDS 1 on NMDS 3 (B). On both plots, species are differentiated according to their section membership. The fossil scales of *S. macracantha*, *S. nyaardii*, *S. recurvata*, and *S. cronbergiae* with unknown phylogenetic classification are added into the ordination diagram. The morphological variables strongly correlated with NMDS axes ( $R^2 > 0.7$ ) are shown in (C) and (D), corresponding to plots (A) and (B), respectively.

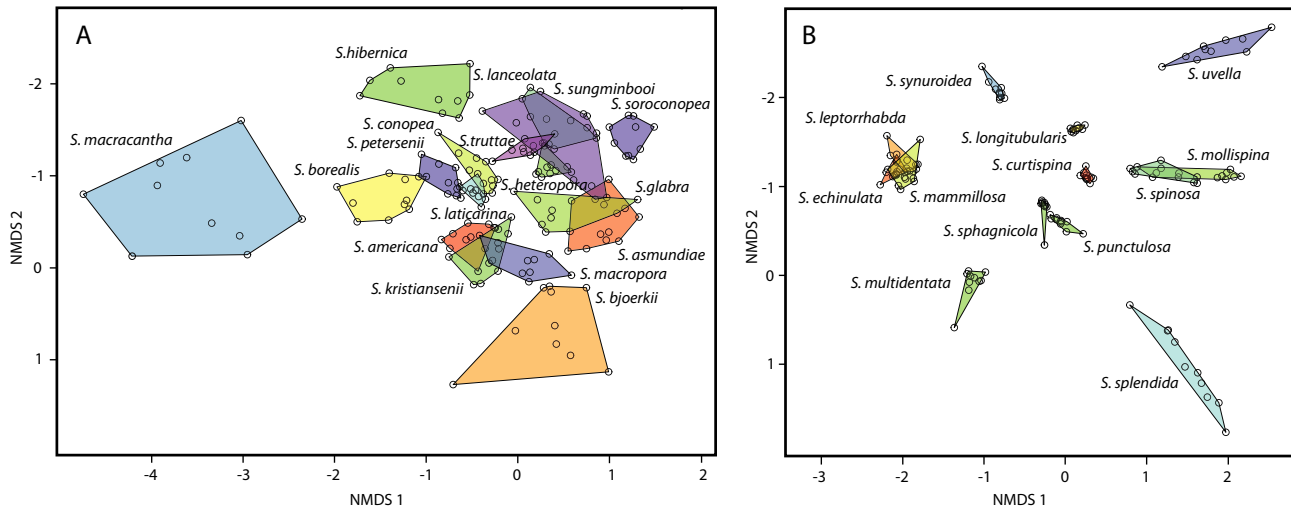


FIG. 5. Morphological comparisons of 30 characters measured on ten body scales per *Synura* species. The ordination diagrams (NMDS) were produced separately for the species with median keel (A) and with spine (B) on their scales, respectively. The fossil scales were removed from the analyses due to the lack of specimens (less than 10 scales per taxa).

In order to trace changes in scale morphology over time, non-correlated morphological traits (Table S2) were mapped directly onto the phylogenetic tree (Figs. 6, 7, S1 in the Supporting Information). Some morphological characters, including formation of the keel (section *Petersenianae*) and the labyrinth pattern found in *Synura leptorrhabda*, *S. mammillosa*, *S. echinulata* (Figs. 3, S1, A and B), clearly evolved once. Other features, such as the meshwork pattern in *S. spinosa*, *S. mollispina*, *S. longitubularis*, *S. curtispina*, and *S. uvella* (Figs. 3, S1C) appeared multiple times in the evolution of the genus.

Other trends in the shapes and the sizes of specific structures were noted. Scale roundness and circularity were greatest in more basal lineages, and especially declined in recent crown lineages within section *Petersenianae* (Fig. 6, A and D). The width of the upturned rim also tended to decline in recent lineages within section *Petersenianae* (Figs. 6F, S1E). Interestingly, the longest scales were produced by some of the more ancestral species inferred at the base of both the *Petersenianae* and *Synura* + *Curtispinae* sections, as noted in the lineages represented by *S. macracantha*, *S. uvella*, and *S. splendida*, respectively (Fig. 6C). In addition, the upturned rim encircled a larger percentage of the scale perimeter in the ancestral section *Curtispinae* lineage and gradually less of the perimeter during evolution of most taxa within section *Petersenianae* (Fig. 6, E and F). Larger base plate holes evolved in species with a keel (Fig. 7C), while species with spine-bearing scales tended to evolve larger base plate pores than those found on scales with a keel (Fig. 7A). *Synura macracantha*, at the base of section *Petersenianae*, has the longest keel with the highest number of attached ribs (Fig. 7D). The length of the

diverticulum forming the spine or the keel was found to be quite variable (Fig. 7E), while a wider width of the diverticulum clearly evolved within species with a keel (Fig. 7F).

#### DISCUSSION

*Phylogenetic assessment of the genus Synura.* Since the 18th century, organisms with similar morphologies have often been considered to be evolutionary closely related, descendants of a common ancestor. Such is the case for *Synura*, as the phylogenetic relationships based on molecular analyses are mirrored in the morphological similarity of their silica scales (Fig. 3). *Synura* is divided into two dominant groups based on species possessing scales with either a median keel or a forward projecting spine, a character trait well supported by molecular data. Such a morphological distinction supports the division of the genus into two sections *Petersenianae* and *Spinosae*, originally proposed by Petersen and Hansen (1956), and later revised as section *Petersenianae* and section *Synura* by Siver et al. (2015). More recently, Jo et al. (2016) proposed a third section, splitting section *Synura* into sections *Synura* and *Curtispinae*. Under this framework, section *Synura* contains *S. uvella*, and section *Curtispinae* all other species with spine-bearing scales. In our study, additional clusters of species with similar scale characters can be traced within the phylomorphospace, indicating an even finer separation of taxa bearing scales with spines as proposed by Škaloud et al. (2013). In a few cases, it has been more difficult to separate closely related taxa using scale morphology, for example, among a number of *Petersenianae* species (Fig. 5A) or closely related strains of *S. mammillosa*, *S. echinulata*, and *S. leptorrhabda* (Fig. 5B). This problem has been

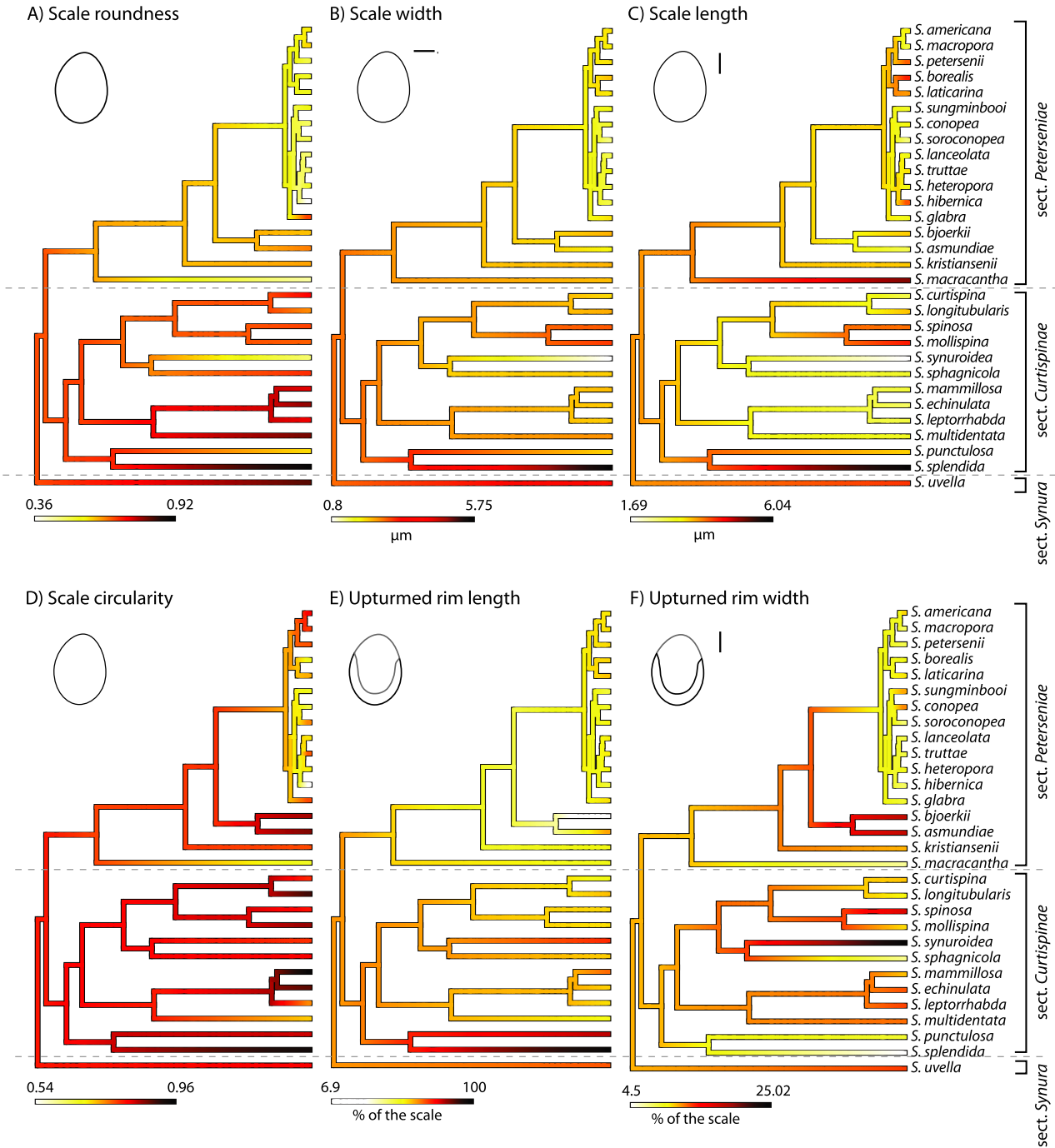


FIG. 6. Evolution of selected morphological characters mapped onto the phylogenetic tree inferred by the BEAST analysis: (A) scale roundness, (B) scale length ( $\mu\text{m}$ ), (C) scale width ( $\mu\text{m}$ ), (D) scale circularity, (E) upturned rim length (% of the scale), and (F) upturned rim width (% of the scale).

aided by adding some morphological characters not previously used in delineating between species (Skaloud et al. 2014).

Combining the phylogenetic relationships of the species with their morphological traits provides further insights into the evolution of the genus *Synura*. Wee (1997) depicted a phylogenetic tree using scale

development and morphological traits. He suggested that the most ancestral scales were those with bilateral symmetry and lacking secondary structures (such as *S. sphagnicola* and *S. splendida*). In addition, according to Wee (1997) and Lavau et al. (1997), *S. uvella* should be closely related to *S. spinosa* and *S. curtispina*. However, molecular studies presented

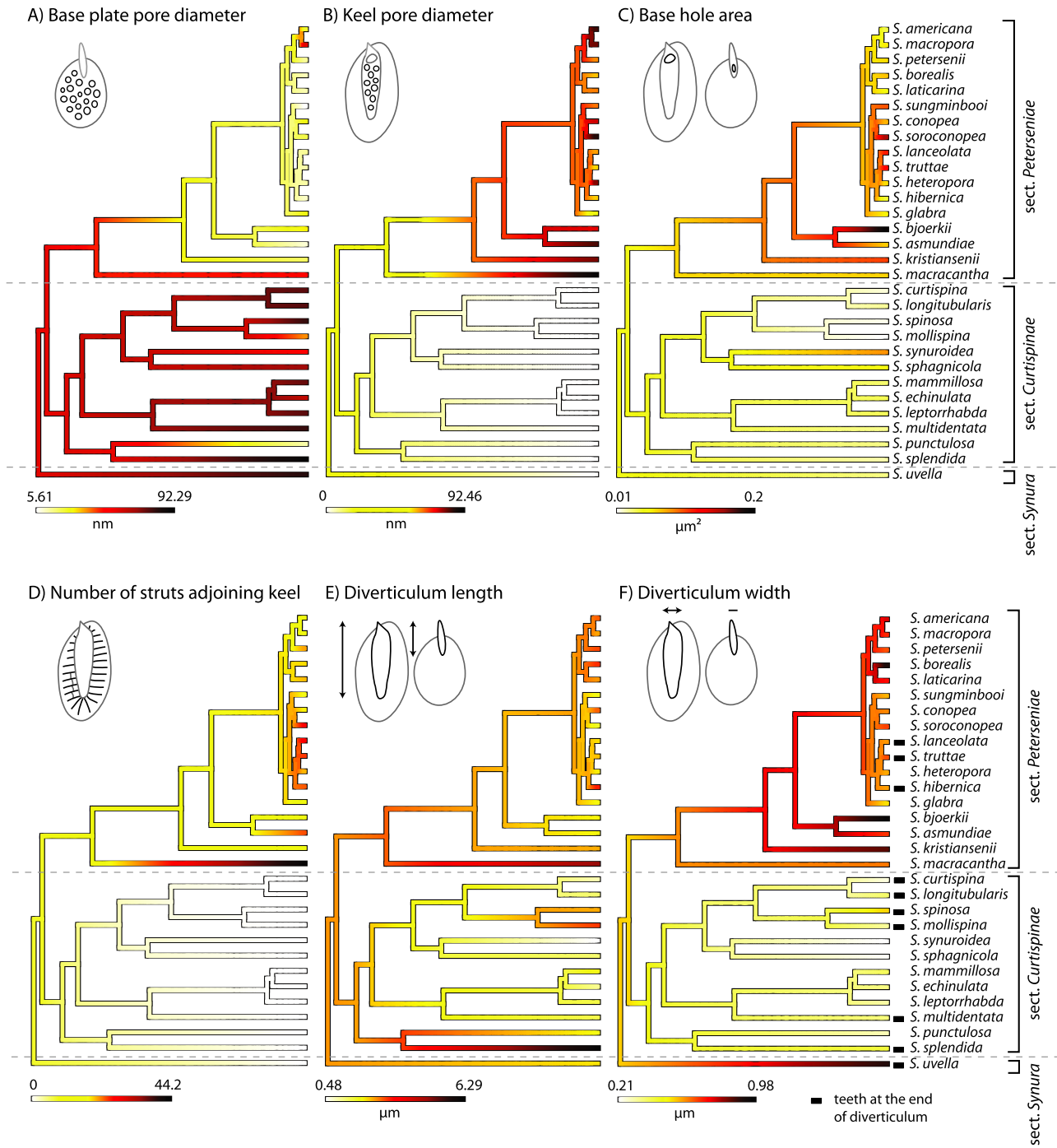


FIG. 7. Evolution of selected morphological characters mapped onto the phylogenetic tree inferred by the BEAST analysis: (A) base plate pore diameter (nm), (B) keel pore diameter (nm) and (C) base hole area ( $\mu\text{m}^2$ ), (D) number of struts adjoining keel, (E) diverticulum (median keel or spine) length ( $\mu\text{m}$ ), and (F) diverticulum (median keel or spine) width ( $\mu\text{m}$ ); the black boxes at the end of branches indicate teeth/split ends of the diverticulum.

by Siver et al. (2015), Jo et al. (2016), and confirmed in our study, indicate that *S. uvella* represents the most ancestral species in the genus. In addition, we found *S. sphagnicola* to be related to species possessing a meshwork on their scales (*S. mollispina*, *S. spinosa*, *S. curtispina*, and *S.*

*longitubularis*). Consequently, we consider the simple appearance of a *S. sphagnicola* scale as an evolutionary simplification of a more complex scale that possessed a meshwork type of ornamentation.

Our multigene phylogenetic tree (Fig. 3) is highly congruent with the analyses of Siver et al. (2015)

and Jo et al. (2016), with a few minor modifications. The phylogenetic position of *Synura punctulosa* with its morphologically unique scales was previously unknown and thought to possibly represent a separate section of the genus (Škaloud et al. 2013). Although scales of *S. punctulosa* possess a spine, they have exceptionally small base plate perforations, less rounded scales than other spine-bearing species, and possess a unique pattern of anatomizing ribs across the scale surface. Our molecular analyses place *S. punctulosa* together with *S. splendida* at the base of section *Curtispineae* as formerly proposed by Jo et al. (2016), and separating from other members of section *Curtispineae*, as well as from each other, in the Upper Cretaceous. Scales of *Synura punctulosa* and *S. splendida* have a simple appearance of the base plate with small perforations, and a longer than average upturned rim. We hypothesize that in the course of evolution, *S. splendida* invested into enlarging its scales and the spine, while *S. punctulosa* strengthened its scales with ribs.

*Scale architectural principles.* Scales are fit into a highly organized pattern that effectively covers the changing contour of the cell. They are positioned in spiral overlapping rows that are oriented at an angle with respect to the longitudinal axis of the cell. Each spiral row contains a few apical scales, mostly body scales, and ends with caudal scales. Although the largest variations in scale structure are with the apical and caudal scales found on the ends of the cell, only slight and less pronounced changes occur among the body scales that surround the majority of the cell. Body scales are slightly concave and more or less bilaterally symmetric (Leadbeater 1986). The left side of the upturned rim is often slightly longer than the right side, perhaps to accommodate the tilting of the spiral rows around the cell.

Each scale is formed endogenously within a specialized vesicle, the silica deposition vesicle (SDV). The process by which the SDV is involved in scale biogenesis was demonstrated first by Greenwood (1967), followed by a number of works each adding to our understanding of scale development (Schnep and Deichgräber 1969, McGrory and Leadbeater 1981, Mignot and Brugerolle 1982, Brugerolle and Bricheux 1984, Leadbeater 1984, Sandgren et al. 1996). The collection of studies demonstrated that during scale biogenesis, the SDV originates near the anterior and outer surface of one plastid, and becomes attached to the periplastid endoplasmic reticulum (PER) with a series of microtubules. The SDV is then molded into the shape of a scale as it is moved down and along the outer surface of the plastid by the microtubules. Once molded into final shape, amorphous silica is deposited and polymerized forming the finished scale. During the molding process, an invagination of the SDV referred to as the cytoplasmic diverticulum is made, marking the position of the base pore and used to form either

the median keel or the projecting spine. If the invagination bends forward and away from the body of the SDV, it will form a spine. In contrast, if it bends backwards and comes to rest on the SDV it will form a keel.

The size of the base plate hole is related to the size, and most likely the width, of the spine or keel that it forms (Fig. 7C). Because the keel comes to rest on and fuses to the base plate, it strengthens the scale which, in turn, decreases potential breakage. The proportions of the keel tip are highly variable among section *Petersenianae* species (Fig. 2, N-AD). There are taxa with either very short (*Synura truttae*, *S. lanceolata*, *S. heteropora*) or very wide keel tips (*S. bjoerkii*, *S. borealis*, *S. asmundiae*, *S. kristiansenii*). However, keel tip length is significantly correlated with scale width, suggesting an architectural constraint in scale construction. Although the reason remains unclear, pores associated with the keel are always larger than those on the base plate.

Siliceous ribs on the scale surface can also serve to strengthen the scale. The number of ribs, or struts, that radiate from the keel onto the base plate was negatively correlated with the roundness of the scale. Thus, species with less rounded scales, such as *Synura macracantha*, possessed a high number of struts (Fig. 7D). The struts that radiate from the keel are likely produced from extensions of the portion of the diverticulum that comes to rest on the base plate. It is interesting that spine-bearing taxa may also form short ribs emanating from the base of the spine near the base hole where the diverticulum is connected to the scale. These short ribs, especially visible on *S. splendida*, were pointed out by Nicholls and Gerrath (1985), and later proposed to be homologous to the struts radiating from the keel (Wee 1997). Other ribs, such as those forming a labyrinth pattern (e.g., *S. mammosa*, *S. echinulata*, and *S. leptorrhabda*), a hexagonal meshwork (e.g., *S. mollispina*, *S. curtispina*, and *S. spinosa*), those under the upturned rim of *S. uvella*, as well as the ribs on *S. punctulosa*, are probably directly formed by the main portion of the SDV producing the base plate.

For many spine-bearing species, the anterior portion of the scale contains secondary structure, whereas the posterior part within the confines of the upturned rim may not. The upturned rim is associated with a portion of the SDV that bends up and over the base plate. Moreover, the outer surface of the rim is coated with an organic adhesive substance which aids to cement the scales in place on the cell surface (Leadbeater 1986, 1990, Beech et al. 1990). The upturned rim may serve to precisely align the scales in a similar manner to the V-rib in *Mallomonas* scales (Siver and Glew 1990). The length of the upturned rim has also been shown to vary with the degree of secondary structure found on the anterior portion of the scale (Gutowski 1996, Němcová et al. 2010). For example, Němcová et al. (2010) reported an increase in the percentage of

the scale margin covered by the upturned rim in *Synura echinulata* concurrent with a reduction in the labyrinth ribbing pattern when grown under increasing temperatures. This suggests that the upturned rim may compensate for a reduction in secondary structures, perhaps to help maintain scale strength. Because the length of the upturned rim was correlated with the area and perimeter of the scale, the length of the spine, and the length of the keel, we further conclude that it represents an evolutionary conservative feature. It is interesting to note that silica scale-bearing chrysophytes may have an advantage over other groups of eukaryotes that form cell coverings out of silica (e.g., diatoms) in that even though  $\text{Si}(\text{OH})_4$  is needed for scale production, it is not essential for cell growth (Sandgren et al. 1996). In culture studies where silica was depleted, cells initially formed less silicified scales, then aberrant formed scales, and eventually cells lacking scales altogether (Klaveness and Guillard 1975, Sandgren et al. 1996).

*Evolution trends of Synura scale case.* Intracellular deposition of silica is common in eukaryotes, occurring in cercozoa, alveolates, amoebzoa, rhizaria, archaeplastida, and stramenopiles (Marron et al. 2016). Many hypotheses have been proposed to explain the potential benefits of a siliceous cell covering. First, it may relate to conserving resources since it requires more energy to build a polysaccharide cell wall than a silica scale case (Raven 1983). Second, the scales are evenly silicified and regularly perforated, which may increase light diffraction into the cell interior and simultaneously increase photosynthetic efficiency (De Tommasi et al. 2010). Third, the siliceous scales may contribute to reducing dangerous UV-B and UV-A radiation reaching the cell interior (Beardall and Raven 2004, De Stefano et al. 2007, Bismuto et al. 2008). Fourth, the silica scale case may serve to protect against grazing and parasitism, although a wide range of organisms are able to overcome such a barrier (Raven and Waite 2004, Spillane 2016, Pančić et al. 2019). For example, some viruses are capable of penetrating through pores about 0.1  $\mu\text{m}$  wide, and others may use an enzymatic digestion of the organic cement to disrupt the scale case (Brussaard 2004, Metreveli et al. 2014, Herringer et al. 2019). The reduction in scale pore size observed over the evolution of the genus *Synura* (Figs. 7, A and B, S1F), may have been a response to improving the protective barrier against viruses and parasites.

The reduction in pore size could also be a function of the concurrent reduction in cell size reduction observed over geologic time. The oldest lineages of both spine and keel-bearing *Synura* species (e.g., *Synura splendida* and *S. macracantha*) have bigger scales than more recently diversified lineages (Fig. 6, A and B). Indeed, scales of the extinct species *S. cronbergiae* and fossil specimens of *S. macracantha* uncovered from the Giraffe core possessed

large scales compared with modern taxa (Siver et al. 2013a). Perhaps, cells reduced the mass of heavier scales by producing bigger pores, as a method to reduce the energy needed by the cell to remain near the surface and to help prevent it from sinking out of the euphotic zone. Smaller cells with smaller scales were also thought to be related to the global warm temperatures found during the Paleocene–Eocene Epochs (Siver et al. 2015). This hypothesis was based on the general temperature-size rule proposed for protists (Atkinson et al. 2003), as well as on short-term studies of chrysophytes in culture (Pichrtová and Němcová 2011).

In addition to pore size, other traits that are associated with the scale case can be traced during the evolution of the genus. Scales have become less round, partially due to the formation of the keel for species in section *Petersenianae* (Fig. 6, A and D). More elongated scales might fit easier around elongated cells with reduced volume to surface ratio, which are selected by the competition for nutrients (Karp-Boss and Boss 2016). Based on previous phylogenetic analyses (e.g., Siver et al. 2015, Škaloud et al. 2020), and confirmed in our study, evolution of the median keel occurred only once. Interestingly, despite the fact that the keel on fossil *Synura macracantha* scales from Eocene deposits has a series of perforations along the sides, it remained well secured to the scale surface (Siver 2013). In addition, *S. macracantha* has the longest known keel with the highest number of struts among *Synura* taxa (Fig. 2N). Keel length gradually shortened over geologic time (Fig. 7E), concurrent with a decline in the number of struts associated with the keel (Fig. 7D) and scale size, possibly as a consequence of better fitting into the cell covering as cell size decreased.

Although spines are proposed to be advantageous as a defense against predators (van Tol et al. 2012, Pančić and Kiørboe 2018) or to possibly reduce sinking in the water column (Laurenceau-Cornec et al. 2015, Walker 2019), such benefits seem of limited value for *Synura* species, given they are actively swimming colonial flagellates where the spines do not effectively increase the size of the colony. We propose that the benefit of a median keel for reinforcing scale strength is more beneficial for *Synura* than a protruding spine. Indeed, the keel-bearing *Synura* species are often more abundant in water bodies than the spine-bearing taxa (Kiss and Kristiansen 1994, Pichrtová et al. 2007, Kynčlová et al. 2010). In addition, there has been a greater degree of species diversification within section *Petersenianae* than section *Synura* since the late Neogene (Škaloud et al. 2020).

The impact of some morphological scale features on cell fitness is not always clear and may in fact represent a consequence of past evolutionary processes. For example, the upturned rim is longest in the more ancestral *Synura* species, including *S.*

*uwella*, *S. punctulosa*, and *S. splendida* (in this species it even encircles the whole scale; Figs. 6E, S1D), as well as in the extinct species *S. cronbergiae* and *S. recurvata*. Interestingly, the rim also encircles the whole scale of both known species of *Neotessella*, a most ancestral genus of the Synurales (Siver et al. 2015). The precise hexagonal meshwork secondary structure commonly found on modern scales of *S. spinosa*, *S. mollispina*, *S. longitubularis*, *S. curtispina*, and *S. uwella* (Fig. 3C), as well as on scales of fossil specimens of *S. cronbergiae*, *S. recurvata*, *S. nygaardii*, and *S. recurvata* (Siver and Wolfe 2005, Siver et al. 2013a), has remained a stable feature over time. This feature would also strengthen the scale. In fact, *S. cronbergiae*, which has scales mostly covered with a hexagonal meshwork, is imagined to be a possible prototype of the last common ancestor of both spine and keel-bearing *Synura*.

The study was supported by the Czech Science Foundation (project No. 20-22346S), the Charles University (project GA UK No. 1498119), and the United States National Science Foundation (grants EAR-1725265 and EAR-1940070).

- Ankenbrand, M. J., Keller, A., Wolf, M., Schultz, J. & Förster, F. 2015. ITS2 database V: twice as much. *Mol. Biol. Evol.* 32:3030–2.
- Arbour, J. H. & López-Fernández, H. 2013. Ecological variation in South American geophagine cichlids arose during an early burst of adaptive morphological and functional evolution. *Proc. R. Soc. B Biol. Sci.* 280:20130849.
- Asmund, B. 1968. Studies on chrysophyceae from some ponds and lakes in Alaska. VI. Occurrence of *Synura* species. *Hydrobiologia* 31:497–515.
- Atkinson, D., Ciotti, B. J. & Montagnes, D. J. S. 2003. Protists decrease in size linearly with temperature: ca. 2.5% C<sup>-1</sup>. *Proc. R. Soc. B Biol. Sci.* 270:2605–11.
- Balonov, I. M. 1976. Rod *Synura* Ehr. (Chrysophyta). *Biologija, Ekologija, Sistematika. Akad. Nauk. SSSR, Institut Vnutrennich Vod., Trudy.* 31:61–82.
- Beardall, J. & Raven, J. A. 2004. The potential effects of global change on microalgal photosynthesis, growth and ecology. *Phycologia* 43:26–40.
- Beech, P. L., Wetherbee, R. & Pickett-Heaps, J. D. 1990. Secretion and deployment of bristles in *Mallomonas splendens* (Synurophyceae). *J. Phycol.* 26:112–22.
- Bismuto, A., Setaro, A., Maddalena, P., De Stefano, L. & De Stefano, M. 2008. Marine diatoms as optical chemical sensors: A time-resolved study. *Sens. Actuat. B Chem.* 130:396–9.
- Boenigk, J., Pfandl, K. & Hansen, P. J. 2006. Exploring strategies for nanoflagellates living in a 'wet desert'. *Aquat. Microb. Ecol.* 44:71–83.
- Boo, S. M., Kim, H. S., Shin, W., Boo, G. H., Cho, S. M., Jo, B. Y., Kim, J. H. et al. 2010. Complex phylogeographic patterns in the freshwater alga *Synura* provide new insights into ubiquity vs. endemism in microbial eukaryotes. *Mol. Ecol.* 19:4328–38.
- Brugerolle, G. & Bricheux, G. 1984. Actin microfilaments are involved in scale formation of the chryomonad cell *Synura*. *Protoplasma* 123:203–12.
- Brussaard, C. P. 2004. Viral control of phytoplankton populations – a review. *J. Eukaryotic Microbiol.* 51:125–38.
- Castellanos, M. C., Wilson, P., Keller, S. J., Wolfe, A. D. & Thomson, J. D. 2006. Another evolution: pollen presentation strategies when pollinators differ. *Am. Nat.* 167:288–96.
- Castresana, J. 2000. Selection of conserved blocks from multiple alignments for their use in phylogenetic analysis. *Mol. Biol. Evol.* 17:540–52.
- Čertnerová, D., Čertner, M. & Škaloud, P. 2019. Molecular phylogeny and evolution of phenotype in silica-scaled chrysophyte genus *Mallomonas*. *J. Phycol.* 55:912–23.
- Darriba, D., Taboada, G. L., Doallo, R. & Posada, D. 2012. *jModelTest 2*: more models, new heuristics and parallel computing. *Nat. Methods* 9:772.
- De Stefano, L., Rea, I., Rendina, I., De Stefano, M. & Moretti, L. 2007. Lensless light focusing with the centric marine diatom *Coscinodiscus walesii*. *Opt. Express.* 15:18082–8.
- De Tommasi, E., Rea, I., Mocella, V., Moretti, L., De Stefano, M., Rendina, I. & De Stefano, L. 2010. Multi-wavelength study of light transmitted through a single marine centric diatom. *Opt. Express.* 18:12203–12.
- Elmer, K. R., Kusche, H., Lehtonen, T. K. & Meyer, A. 2010. Local variation and parallel evolution: morphological and genetic diversity across a species complex of neotropical crater lake cichlid fishes. *Phil. Trans. R. Soc. B Biol. Sci.* 365:1763–82.
- Endler, J. A. & Day, L. B. 2006. Ornament colour selection, visual contrast and the shape of colour preference functions in great bowerbirds, *Chlamydera nuchalis*. *Anim. Behav.* 72:1405–16.
- Feilich, K. L. 2016. Correlated evolution of body and fin morphology in the cichlid fishes. *Evolution* 70:2247–67.
- Fott, B. & Ludvík, J. 1957. Die submikroskopische Struktur der Kieselschuppen bei *Synura* und ihre Bedeutung für die Taxonomie der Gattung. *Preslia* 29:5–16.
- Gavrilova, O. V., Nogina, N. V. & Voloshko, L. N. 2005. Scale structures and growth characteristics of *Synura petersenii* (Synurophyceae) under different pH conditions. *Nova Hedwig. Beih.* 128:249–56.
- Greenwood, A. D. 1967. Scale production in *Synura*. *Proc. R. Microbiol. Soc.* 2:380–1.
- Gutowski, A. 1996. Temperature dependent variability of scales and bristles of *Mallomonas tonsurata* Teiling emend. Krieger (Synurophyceae). *Nova Hedwig. Beih.* 114:125–46.
- Hartmann, H. & Steinberg, C. 1986. Mallomonadacean (Chrysophyceae) scales: Early biotic paleoindicators of lake acidification. *Hydrobiologia* 143:87–91.
- Hepperle, D. 2004. SeqAssem (C). A sequence analysis tool, contig assembler and trace data visualisation tool for molecular sequences. Available from: [https://www.sequentix.de/software\\_seqassem.php](https://www.sequentix.de/software_seqassem.php).
- Herringer, J. W., Lester, D., Dorrington, G. E. & Rosengarten, G. 2019. Can diatom girdle band pores act as a hydrodynamic viral defense mechanism? *J. Biol. Phys.* 45:213–34.
- Jo, B. Y., Kim, J. I., Škaloud, P., Siver, P. A. & Shin, W. 2016. Multigene phylogeny of *Synura* (Synurophyceae) and descriptions of four new species based on morphological and DNA evidence. *Eur. J. Phycol.* 51:413–30.
- Jo, B. Y., Shin, W., Boo, S. M., Kim, H. S. & Siver, P. A. 2011. Studies on ultrastructure and three-gene phylogeny of the genus *Mallomonas* (Synurophyceae). *J. Phycol.* 47:415–25.
- Karp-Boss, L. & Boss, E. 2016. The elongated, the squat and the spherical: selective pressures for phytoplankton shape. In Glibert, P. M. & Kana, T. M. [Eds.] *Aquatic Microbial Ecology and Biogeochemistry: A Dual Perspective*. Springer, Cham, pp. 25–34.
- Katana, A., Kwiatowski, J., Spalik, K., Zakryś, B., Szalacha, E. & Szymańska, H. 2001. Phylogenetic position of *Koliella* (Chlorophyta) as inferred from nuclear and chloroplast small subunit rDNA. *J. Phycol.* 37:443–51.
- Katoh, K., Rozewicki, J. & Yamada, K. D. 2019. MAFFT online service: multiple sequence alignment, interactive sequence choice and visualization. *Briefings Bioinf.* 20:1160–6.
- Kiss, K. T. & Kristiansen, J. 1994. Silica-scaled chrysophytes (Synurophyceae) from some rivers and shallow lakes in Hungary. *Hydrobiologia* 289:157–62.
- Klavness, D. & Guillard, R. R. 1975. The requirement for silicon in *Synura petersenii* (Chrysophyceae). *J. Phycol.* 11:349–55.
- Kristiansen, J. 1979. Problems in classification and identification of Synuraceae (Chrysophyceae). *Aqua. Sci.* 40:310–19.

- Kristiansen, J. 2008. Dispersal and biogeography of silica-scaled chrysophytes. In Foissner, W. & Hawksworth, D. L. [Eds.] *Prokaryotic Diversity and Geographical Distribution*. Springer, Dordrecht, The Netherlands, pp. 185–192.
- Kristiansen, J. & Preisig, H. R. 2007. Chrysophyte and haptophyte algae, part 2: Synurophyceae. In Budel, B., Gärtner, G., Krienitz, L. & Preisig, H. R. [Eds.] *Süßwasserflora von Mitteleuropa*, vol. 1–2. Springer, Spektrum Akad. Verlag, Berlin, Germany, p. 252.
- Kynčlová, A., Škaloud, P. & Škaloudová, M. 2010. Unveiling hidden diversity in the *Synura petersenii* species complex (Synurophyceae, Heterokontophyta). *Nova Hedwig. Beih.* 136:283–98.
- Laurenceau-Cornec, E. C., Trull, T. W., Davies, D. M., Christina, L. & Blain, S. 2015. Phytoplankton morphology controls on marine snow sinking velocity. *Mar. Ecol. Prog. Ser.* 520:35–56.
- Lavau, S., Saunders, G. W. & Wetherbee, R. 1997. A phylogenetic analysis of the Synurophyceae using molecular data and scale case morphology. *J. Phycol.* 33:135–51.
- Leadbeater, B. S. C. 1984. Silicification of cell walls of certain prokaryotic flagellates. *Phil. Trans. R. Soc. B Biol. Sci.* 304:529–36.
- Leadbeater, B. S. C. 1986. Scale case construction in *Synura petersenii* Korsch. (Chrysophyceae). In Kristiansen, J. & Andersen, R. A. [Eds.] *Chrysophytes: Aspects and Problems*. Cambridge University Press, Cambridge, Massachusetts, pp. 121–31.
- Leadbeater, B. S. 1990. Ultrastructure and assembly of the scale case in *Synura* (Synurophyceae Andersen). *Eur. J. Phycol.* 25:117–32.
- Maia, R., Rubenstein, D. R. & Shawkey, M. D. 2013. Key ornamental innovations facilitate diversification in an avian radiation. *Proc. Natl. Acad. Sci. USA* 110:10687–92.
- Manton, I. 1955. Observations with the electron microscope on *Synura caroliniana* Whitford. *Proc. Leeds Phil. Soc.* 6:306–16.
- Marron, A. O., Ratcliffe, S., Wheeler, G. L., Goldstein, R. E., King, N., Not, F., de Vargas, C. & Richter, D. J. 2016. The evolution of silicon transport in eukaryotes. *Mol. Biol. Evol.* 33:3226–48.
- Martin-Wagenmann, B. & Gutowski, A. 1995. Scale morphology and growth characteristics of clones of *Synura petersenii* (Synurophyceae) at different temperatures. In Sandgren, C. D., Smol, J. P. & Kristiansen, J. [Eds.] *Chrysophyte Algae: Ecology, Phylogeny and Development*. Cambridge University Press, Cambridge, Massachusetts, pp. 345–60.
- McGrory, C. B. & Leadbeater, B. S. C. 1981. Ultrastructure and deposition of silica in the Chrysophyceae. In Simpson, T. L. & Volcani, B. E. [Eds.] *Silicon and Siliceous Structures in Biological Systems*. Springer, New York, NY, pp. 201–30.
- Metreveli, G., Wägberg, L., Emmoth, E., Belák, S., Strømme, M. & Mihranyan, A. 2014. A size-exclusion nanocellulose filter paper for virus removal. *Adv. Healthcare Mater.* 3:1546–50.
- Mignot, J. P. & Brugerolle, G. 1982. Scale formation in chrysomonad flagellates. *J. Ultrastruct. Res.* 81:13–26.
- Miller, M. A., Pfeiffer, W. & Schwartz, T. 2010. Creating the CIPRES Science Gateway for inference of large phylogenetic trees. Proceedings of the Gateway Computing Environments Workshop (GCE), New Orleans, LA, pp. 1–8.
- Němcová, Y., Neustupa, J., Kvíderová, J. & Řezáčová-Škaloudová, M. 2010. Morphological plasticity of silica scales of *Synura echinulata* (Synurophyceae) in crossed gradients of light and temperature—a geometric morphometric approach. *Nova Hedwig. Beih.* 136:21–32.
- Němcová, Y., Nováková, S. & Řezáčová-Škaloudová, M. 2008. *Synura obesa* sp. nov. (Synurophyceae) and other silica-scaled chrysophytes from Abisko (Swedish Lapland). *Nova Hedwigia* 86:243–54.
- Němcová, Y. & Pichrtová, M. 2012. Shape dynamics of silica scales (Chrysophyceae, Stramenopiles) associated with pH. *Fottea*. 12:281–91.
- Nicholls, K. H. & Gerrath, J. F. 1985. The taxonomy of *Synura* (Chrysophyceae) in Ontario with special reference to taste and odour in water supplies. *Can. J. Bot.* 63:1482–93.
- Pančić, M. & Kjørboe, T. 2018. Phytoplankton defence mechanisms: traits and trade-offs. *Biol. Rev.* 93:1269–303.
- Pančić, M., Torres, R. R., Almeda, R. & Kjørboe, T. 2019. Silicified cell walls as a defensive trait in diatoms. *Proc. R. Soc. B Biol. Sci.* 286:20190184.
- Péterfi, L. S. & Momeu, L. 1977. Remarks on the taxonomy of some *Synura* species based on the fine structure of scales. *St. Nat.* 21:15–23.
- Petersen, J. B. & Hansen, J. B. 1956. On the scales of some *Synura* species. *Biol. Medd. Dan. Vid. Selsk.* 23:1–38.
- Pichrtová, M. & Němcová, Y. 2011. Effect of temperature on size and shape of silica scales in *Synura petersenii* and *Mallomonas tonsurata* (Stramenopiles). *Hydrobiologia* 673:1–11.
- Pichrtová, M., Řezáčová-Škaloudová, M. & Škaloud, P. 2007. The silica-scaled chrysophytes of the Czech-Moravian Highlands. *Fottea* 7:43–8.
- Pusztai, M., Čertnerová, D., Škaloudová, M. & Škaloud, P. 2016. Elucidating the phylogeny and taxonomic position of the genus *Chrysodidymus* Prowse (Chrysophyceae, Synurales). *Cryptogam. Algal.* 37:297–307.
- Quesada-Aguilar, A., Kalisz, S. & Ashman, T. L. 2008. Flower morphology and pollinator dynamics in *Solanum carolinense* (Solanaceae): implications for the evolution of andromonoecy. *Am. J. Bot.* 95:974–84.
- R Core Team 2019. *R: A Language and Environment for Statistical Computing*. R Foundation for Statistical Computing, Vienna, Austria.
- Rambaut, A. 2016. FigTree version 1.4.3. Available at: <http://tree.bio.ed.ac.uk> (last accessed 12 October 2020).
- Rambaut, A., Drummond, A. J., Xie, D., Baele, G. & Suchard, M. A. 2018. Posterior summarisation in Bayesian phylogenetics using Tracer 1.7. *Syst. Biol.* 67:901.
- Rasband, W. S. 1997. ImageJ, U. S. National Institutes of Health, Bethesda, Maryland, USA. Available at: <https://imagej.nih.gov/ij/> (last accessed 12 October 2020).
- Raven, J. A. 1983. The transport and function of silicon in plants. *Biol. Rev.* 58:179–207.
- Raven, J. A. & Waite, A. M. 2004. The evolution of silicification in diatoms: inescapable sinking and sinking as escape? *New Phytol.* 162:45–61.
- Revell, L. J. 2012. Phytools: An R package for phylogenetic comparative biology (and other things). *Methods. Ecol. Evol.* 3:217–23.
- Řezáčová-Škaloudová, M., Neustupa, J. & Němcová, Y. 2010. Effect of temperature on the variability of silicate structures in *Mallomonas kalinae* and *Synura curtispina* (Synurophyceae). *Nova Hedwig. Beih.* 136:55–70.
- Ronquist, F., Teslenko, M., Van Der Mark, P., Ayres, D. L., Darling, A., Höhna, S., Larget, B., Liu, L., Suchard, M. A. & Huelsenbeck, J. P. 2012. MrBayes 3.2: efficient Bayesian phylogenetic inference and model choice across a large model space. *Syst. Biol.* 61:539–42.
- Rubenstein, D. R. & Lovette, I. J. 2009. Reproductive skew and selection on female ornamentation in social species. *Nature* 462:786–9.
- Sandgren, C. D., Hall, S. A. & Barlow, S. B. 1996. Siliceous scale production in chrysophyte and synurophyte algae. I. Effects of silica-limited growth on cell silica content, scale morphology, and the construction of the scale layer of *Synura petersenii*. *J. Phycol.* 32:675–92.
- Saxby-Rouen, K. J., Leadbeater, B. S. C. & Reynolds, C. S. 1997. The growth response of *Synura petersenii* (Synurophyceae) to photon flux density, temperature, and pH. *Phycologia* 36:233–43.
- Schnep, E. & Deichgräber, G. 1969. Über die Feinstruktur von *Synura petersenii* unter besonderer Berücksichtigung der Morphogenese ihrer Kieselschuppen. *Protoplasma* 68:85–106.
- Siver, P. A. 1987. The distribution of *Synura* species (Chrysophyceae) in Connecticut, U.S.A. including the description of a new form. *Nordic J. Bot.* 7:107–16.
- Siver, P. A. 2013. *Synura cronbergiae* sp. nov., a new species described from two Paleogene maar lakes in northern Canada. *Nova Hedwigia* 97:179–87.
- Siver, P. A. 2015. The Synurophyceae. In Wehr, J. D., Sheath, R. G. & Kociolek, J. P. [Eds.] *Freshwater Algae of North America:*

- Ecology and Classification*, 2nd edn. Academic Press, San Diego, California, USA, pp. 605–650.
- Siver, P. A. & Glew, J. R. 1990. The arrangement of scales and bristles on *Mallomonas* (Chrysophyceae): a proposed mechanism for the formation of the cell covering. *Can. J. Bot.* 68:374–80.
- Siver, P. A., Jo, B. Y., Kim, J. I., Shin, W., Lott, A. M. & Wolfe, A. P. 2015. Assessing the evolutionary history of the class Synurophyceae (Heterokonta) using molecular, morphometric, and paleobiological approaches. *Am. J. Bot.* 102:921–41.
- Siver, P. A., Kapustin, D. & Gusev, E. 2018. Investigations of two-celled colonies of *Synura* formerly described as *Chrysodidymus* with descriptions of two new species. *Eur. J. Phycol.* 53:245–55.
- Siver, P. A. & Lott, A. M. 2016. Descriptions of two new species of *Synurophyceae* from a bog in Newfoundland, Canada: *Mallomonas baskettii* sp. nov. and *Synura kristiansenii* sp. nov. *Nova Hedwigia* 102:501–11.
- Siver, P. A., Lott, A. M. & Wolfe, A. P. 2013a. A summary of *Synura* taxa in early Cenozoic deposits from Northern Canada. *Nova Hedwig. Beih.* 142:181–90.
- Siver, P. A. & Wolfe, A. P. 2005. Eocene scaled chrysophytes with pronounced modern affinities. *Int. J. Plant Sci.* 166:533–6.
- Siver, P. A., Wolfe, A. P., Rohlf, F. J., Shin, W. & Jo, B. Y. 2013b. Combining geometric morphometrics, molecular phylogeny, and micropaleontology to assess evolutionary patterns in *Mallomonas* (Synurophyceae: Heterokontophyta). *Geobiology* 11:127–38.
- Škaloud, P., Kristiansen, J. & Škaloudová, M. 2013. Developments in the taxonomy of silica-scaled chrysophytes—from morphological and ultrastructural to molecular approaches. *Nord. J. Bot.* 31:385–402.
- Škaloud, P., Kynčlová, A., Benada, O., Kofroňová, O. & Škaloudová, M. 2012. Toward a revision of the genus *Synura*, section *Petersenianae* (Synurophyceae, Heterokontophyta): morphological characterization of six pseudo-cryptic species. *Phycologia* 51:303–29.
- Škaloud, P., Škaloudová, M., Jadrná, I., Bestová, H., Pusztai, M., Kapustin, D. & Siver, P. A. 2020. Comparing morphological and molecular estimates of species diversity in the freshwater genus *Synura* (Stramenopiles): a model for understanding diversity of eukaryotic microorganisms. *J. Phycol.* 56:574–91.
- Škaloud, P., Škaloudová, M., Procházková, A. & Němcová, Y. 2014. Morphological delineation and distribution patterns of four newly described species within the *Synura petersenii* species complex (Chrysophyceae, Stramenopiles). *Eur. J. Phycol.* 49:213–29.
- Škaloudová, M. & Škaloud, P. 2013. A new species of *Chrysosphaerella* (Chrysophyceae: Chromulinales), *Chrysosphaerella rotundata* sp. nov., from Finland. *Phytotaxa* 130:34–42.
- Spillane, T. 2016. Diatom frustules as a mechanical defense against predation by heterotrophic dinoflagellates. Master thesis, Western Washington University, 61 pp.
- Stamatakis, A. 2014. RAxML version 8: a tool for phylogenetic analysis and post-analysis of large phylogenies. *Bioinformatics* 30:1312–3.
- Starmach, K. 1985. Chrysophyceae und Haptophyceae. In Ettl, H., Gerloff, J., Heynig, H. & Mollenhauer, D. [Eds.] *Süßwasserflora von Mitteleuropa 1*. VEB Gustav Fischer, Jena, 515 pp.
- Suchard, M. A., Lemey, P., Baele, G., Ayres, D. L., Drummond, A. J. & Rambaut, A. 2018. Bayesian phylogenetic and phylodynamic data integration using BEAST 1.10. *Virus Evol.* 4:vey016.
- Tamura, K., Peterson, D., Peterson, N., Stecher, G., Nei, M. & Kumar, S. 2011. MEGA5: molecular evolutionary genetics analysis using maximum likelihood, evolutionary distance, and maximum parsimony methods. *Mol. Biol. Evol.* 28:2731–9.
- van Tol, H. M., Irwin, A. J. & Finkel, Z. V. 2012. Macroevolutionary trends in silicoflagellate skeletal morphology: the costs and benefits of silicification. *Paleobiology* 38:391–402.
- Walker, M. 2019. Linking shape and sinking speed in planktonic Foraminifera. PhD dissertation, University of Lincoln, UK, 292 pp.
- Wee, J. L. & Andersen, R. A. 1997. Scale biogenesis in synurophycean protists: phylogenetic implications. *Crit. Rev. Plant Sci.* 16:497–534.
- Whittall, J. B. & Hodges, S. A. 2007. Pollinator shifts drive increasingly long nectar spurs in columbine flowers. *Nature* 447:706–9.
- Yoon, H. S., Hackett, J. D. & Bhattacharya, D. 2002. A single origin of the peridinin-and fucoxanthin-containing plastids in dinoflagellates through tertiary endosymbiosis. *Proc. Natl. Acad. Sci. USA* 99:11724–9.

### Supporting Information

Additional Supporting Information may be found in the online version of this article at the publisher's web site:

**Figure S1.** Evolution of selected morphological characters mapped onto the phylogenetic tree inferred by BEAST analysis: (A) median keel with struts, (B) labyrinthic pattern, (C) meshwork pattern, (D) upturned rim length ( $\mu\text{m}$ ), (E) upturned rim width ( $\mu\text{m}$ ) and (F) base plate pore diameter (without pores under meshwork) (nm).

**Table S1.** List of strains used for the phylogenetic analyses, along with the geographical origin and the GenBank accession numbers for nu SSU rDNA, nu LSU rDNA, nu ITS rDNA, pt LSU rDNA, pt *rbcL*, and pt *psaA* sequences. Newly obtained sequences are given in bold. DNA alignments are freely available on Mendeley Data: <http://dx.doi.org/10.17632/rh2tzgf7pz.1>.

**Table S2.** Complete list with average values of evaluated scale characteristics of thirty selected *Synura* species.

**Table S3.** The correlation matrix of scale morphological characteristics obtained by Spearman analyses. Traits with index 0.8 or higher were assessed as correlated and excluded from subsequent phylogenetic analyses.